

FOLLOWING THE REACTION OF CHEMICAL WARFARE AGENTS
ON ADSORBENTS BY
TRANSMISSION FOURIER INFRARED SPECTROMETRY

J. Michael Lochner and Philip W. Bartram
Research & Technology Directorate, Edgewood Chemical – Biological Center, APG, MD

ABSTRACT

The reactions of HD, VX, and GD on metal oxides and core-shell metal oxides were followed by transmission FTIR. The decomposition was determined by the decrease in characteristic absorption peaks noted for each agent. The increase in the characteristic absorption peaks for hydrolysis products was also used to verify the reactions. Typical absorbance bands for agent and major hydrolysis product were as follows: GD (1320 cm^{-1}) and PMPA (1189 cm^{-1}), HD (1295 cm^{-1} and 1212 cm^{-1}) and TDG (1059 cm^{-1}), VX (1299 cm^{-1}) and EMPA (1315 cm^{-1}). Two different samples of aerogel prepared magnesium oxide (AP-MgO) demonstrated significant GD reactivity over 20 hours at room temperature. Little or no agent decomposition occurred on the other adsorbents. The work supported the Destructive Adsorption program.

INTRODUCTION

Immediate decontamination includes three procedures, personal wipe down, operator's wipe down or operator's spray down, and application to skin.¹ Almost exclusively the U.S. Army procedures have been limited to adsorbents. The Applied Chemistry Team, Edgewood Chemical-Biological Center, began a sorbent program in FY99 to develop the next generation of reactive adsorbent to replace aluminum oxide in immediate decontamination procedures. The major approach was to prepare and evaluate nanocrystallite metal oxides, and core-shell metal oxides. Kansas State University^{2,3} and Clark Atlanta University⁴ have reported several adsorbents that demonstrated fast reactivity towards dimethyl methylphosphonate (DMMP). Because some of the adsorbents were paramagnetic, kinetics could not be determined using Solid State NMR. Therefore, a Fourier Transform Infrared (FTIR) technique was developed to follow the reactions of HD, VX, and GD on the adsorbents.

In this report, we will describe the FTIR method used to evaluate the reactivity of paramagnetic core-shell adsorbents and diamagnetic nanocrystallite adsorbents, and document the kinetics and extent of reaction of HD, VX, and GD on these materials.

MATERIALS

Pinacolyl methylphosphonofluoridate (GD), GD-U-2323-CTF-N, purity 98.8%;
Pinacolyl methylphosphonic acid (PMPA), 87-0022-74-1, purity 83.9%; Bis (2-chloroethyl)

Report Documentation Page				Form Approved OMB No. 0704-0188	
Public reporting burden for the collection of information is estimated to average 1 hour per response, including the time for reviewing instructions, searching existing data sources, gathering and maintaining the data needed, and completing and reviewing the collection of information. Send comments regarding this burden estimate or any other aspect of this collection of information, including suggestions for reducing this burden, to Washington Headquarters Services, Directorate for Information Operations and Reports, 1215 Jefferson Davis Highway, Suite 1204, Arlington VA 22202-4302. Respondents should be aware that notwithstanding any other provision of law, no person shall be subject to a penalty for failing to comply with a collection of information if it does not display a currently valid OMB control number.					
1. REPORT DATE 01 JUL 2003		2. REPORT TYPE N/A		3. DATES COVERED -	
4. TITLE AND SUBTITLE Following The Reaction Of Chemical Warfare Agents On Adsorbents By Transmission Fourier Infrared Spectrometry				5a. CONTRACT NUMBER	
				5b. GRANT NUMBER	
				5c. PROGRAM ELEMENT NUMBER	
6. AUTHOR(S)				5d. PROJECT NUMBER	
				5e. TASK NUMBER	
				5f. WORK UNIT NUMBER	
7. PERFORMING ORGANIZATION NAME(S) AND ADDRESS(ES) Research & Technology Directorate, Edgewood Chemical Biological Center, APG, MD				8. PERFORMING ORGANIZATION REPORT NUMBER	
9. SPONSORING/MONITORING AGENCY NAME(S) AND ADDRESS(ES)				10. SPONSOR/MONITOR'S ACRONYM(S)	
				11. SPONSOR/MONITOR'S REPORT NUMBER(S)	
12. DISTRIBUTION/AVAILABILITY STATEMENT Approved for public release, distribution unlimited					
13. SUPPLEMENTARY NOTES See also ADM001523., The original document contains color images.					
14. ABSTRACT					
15. SUBJECT TERMS					
16. SECURITY CLASSIFICATION OF:			17. LIMITATION OF ABSTRACT UU	18. NUMBER OF PAGES 9	19a. NAME OF RESPONSIBLE PERSON
a. REPORT unclassified	b. ABSTRACT unclassified	c. THIS PAGE unclassified			

sulfide (HD), HD-U-9040-CTF-N (VIAL 3), purity 98.2%; Thiodiglycol (TDG), Eastman Chemical Company, Inc., purity 93.3%; O-Ethyl-S- (2-isopropyl-aminoethyl) methylphosphonothiolate (VX), VX-U-2128-CTF-N (VIAL 179), purity 90.4%; Diisopropylamino ethanol (DIPEA), laboratory sample; Diisopropylamino ethanethiol (RSH), laboratory sample; Ethyl methylphosphonothioic acid (EMPTA), laboratory sample; ethanol (EtOH), laboratory sample; EA2192, laboratory sample, and Ethyl methylphosphonic acid (EMPA), laboratory sample.

Professor Kenneth Klabunde, Kansas State University, supplied the following adsorbents under contractual (Army Research Office contract # DAAD19-00-1-0055) agreement: AP-MgO(1), surface area 586 m²/g, and AP-MgO(2), surface area 400 m²/g, both sorbents were aerogel prepared nanosize magnesium oxide; [Fe₂O₃]MgO (surface area 450 m²/g), a nanosize (AP-MgO) magnesium oxide with about 1 mol % Fe₂O₃ coating; and AP-CaO (surface area 158 m²/g), a nanosize calcium oxide prepared by the sol-gel method. The crystallite size of the nanoparticles is about 4-5 nanometers (nm). Professor Mark Mitchell, Clark Atlanta University, supplied the following adsorbents: [CuO]Al₂O₃ (12.3 wt% CuO on γ -aluminum oxide with a surface area of 148 m²/g), and [Fe₂O₃] Al₂O₃ (surface area 126 m²/g, 8% (w:w) Fe). The crystallite γ -aluminum oxide support had a diameter of approximately 100 nm. Magnesium oxide was obtained from Aldrich (98% MgO, 24,338-8). The adsorbents were tested as received except where otherwise noted.

EXPERIMENTAL PROCEDURE

Chemical agent (VX, GD, and HD) and reaction product standards (50 % w:w) were made up in carbon tetrachloride or chloroform (depending on the solubility). The absorption spectra were recorded between 4000 cm⁻¹ and 600 cm⁻¹ as percent transmission versus wavenumber using a Nicolet 800 Bench spectrophotometer equipped with a MCT-A (mercury-cadmium-telluride) detector (11,700 - 600 cm⁻¹) and a Nicolet 680 Workstation. The spectra were converted to absorbance spectra for analysis and comparison procedures, using the Nicolet 680 Workstation. All measurements were made at 4 cm⁻¹ spectral resolution. The digitized data were stored on the 680 Workstation and on diskettes. Spectra were gathered and compared to note the appearance of peaks that would designate the formation of reaction products from the decomposition of agent on the adsorbent. The disappearance of agent peaks designated the breaking of a bond (reactivity).

A baseline spectrum was generated for each adsorbent. Areas of low absorption for each of the uncontaminated adsorbents were noted. These areas were used to follow the reaction kinetics. The area of interest chosen was the range 1440 cm⁻¹ to 650 cm⁻¹. Additional baseline spectra were acquired for the following neat materials: GD, PMPA, HD, TDG, VX, DIPEA, RSH, and EMPTA.

A solution of agent was applied to the adsorbent using a 10 μ L Hamilton syringe. Initially, 3 μ L of solvent was drawn into the syringe followed by 1 μ L of air. Next, 3 μ L of the agent solution was drawn into the same syringe, followed by 1 μ L of air, and then followed by 1 additional μ L of solvent. The syringe was placed aside. Approximately 3.5 mg of the oxide was placed onto the center of one of the horizontally positioned Cesium Iodide windows (25 mm in diameter). The syringe was then slowly emptied uniformly onto the adsorbent. The second Cesium Iodide window was then placed onto the top of the bottom Cesium Iodide window, and the top window was rotated one full turn to spread the mixture into a thin film, coating the inside areas of the windows. A thin piece of parafilm was stretched around the sides of the windows to

seal the two windows together, but avoiding the transmission area of the windows themselves. The window “sandwich” was then placed in a FTIR cell holder and positioned in the Nicolet 800 analysis chamber for analysis.

Spectra were recorded at “zero” time and every hour thereafter for approximately 20 hours. A MACRO was written to acquire the spectra and store the data. The MACRO is provided in Appendix A. The spectra were compared to determine any increase in peaks due to the formation of decomposition products, and any decrease in peaks due to the decomposition of the agent.

RESULTS

The decomposition of GD was relatively fast on AP-MgO(1), in 14 h the GD-acid/GD ratio changed approximately 5.1 (Figure 1). AP-MgO(1) was considerably more reactive than the Aldrich MgO, which had a change of only 0.38 (GD-acid/GD ratio) in 20 h. Selected spectra for the reaction of GD on AP-MgO(1) at $t = 0$ and 240 min are provided in Figures 3a and 3b, respectively. In Figure 3a, peaks at 789 and 759 cm^{-1} were attributed to CCl_4 . The spectra are also characterized by the GD absorbance peak (1317 cm^{-1}), and a small unknown peak (1211 cm^{-1}), which was possibly the P(O) absorbance band of PMPA. In Figure 3b, the CCl_4 peaks have disappeared due to evaporation. Between 1148 and 1231 cm^{-1} , there appeared to be two peaks, a broad peak due to PMPA ($\sim 1140 \text{ cm}^{-1}$) and the unknown peak at 1212 cm^{-1} .

However, when the experiment was repeated no GD decomposition was detected on AP-MgO(1). The reactions were run months apart and it was assumed that exposure to air had decreased the reactivity of AP-MgO(1). A sample of AP-MgO(1) was then conditioned at 120 °C for 24 hours and then tested. The results are provided in Figure 2. There was no decrease in the peak height attributed to P-F absorbance, which indicated no decomposition had occurred.

The quasi-kinetics for the reaction of GD on a second batch of magnesium oxide, AP-MgO(2), was determined. The decomposition of GD was initially very fast with a GD-acid/GD ratio change of 5.0 in 5 h. The reaction either began to slow or was complete; the GD-acid/GD ratio was only 6.0 at 12 hours and 6.5 after 19 hours. The reactivity of AP-MgO(2) was considerably more reactive than AP-MgO(1) during the first 13 hours of the experiments, and also more reactive than the Aldrich MgO and the other sorbents. Selected spectra for the reaction with GD ($t = 0$ and 240 min) are provided in Figures 3c and 3d, respectively. In Figure 3c, two broad peaks of strong intensity attributed to CCl_4 were again seen at 787 and 760 cm^{-1} . The GD absorbance peak (1318 cm^{-1}) further characterized the spectra, and a significant PMPA peak observed at 1189 cm^{-1} , which indicated that the reaction was proceeding quickly. In Figure 3d, an absorbance band of strong intensity was seen for PMPA. The PMPA band appeared to be masking an upscale unknown peak noted previously in Figure 3c. At $t = 240$ min, no GD was observed. The reaction data (single run) corresponding to P-F absorbance are shown in Figure 2. The height due to the P-F bond absorbance decreased quickly during the first 8 to 9 hours of the reaction from 3.1 to 1.4 absorbance units.

The reaction on $[\text{Fe}_2\text{O}_3]\text{MgO}$ was relatively slow, a change of about 1.5 GD-acid/GD ratio in 19 h (Figure 1), compared to AP-MgO(1). Decomposition was also detected in replicate experiments (Figure 2), a small decrease in peak height occurred over 16 hours.

Some decomposition occurred on the Adrich MgO as determined by the deviation of the data from vertical. The change of GD to GD-acid was only 0.38 in 20 h (Figure 1). No further GD experiments were done with this MgO.

Very little decomposition of GD was seen on $[\text{CuO}]\text{Al}_2\text{O}_3$, the ratio of hydrolysate (PMPA) to GD changed approximately 0.75 over 19 h (Figure 1). When the reaction was followed by P-F peak height, no decomposition was seen over 20-hours (Figure 2).

There was no decomposition of GD on $[\text{Fe}_2\text{O}_3]\text{Al}_2\text{O}_3$ over 19 h at 25 °C. The lack of reaction is evident from the vertical slopes obtained from the change of GD-acid with time (Figure 1). There was also no evidence of C-P bond cleaving in GD on $[\text{Fe}_2\text{O}_3]\text{Al}_2\text{O}_3$. Cleavage of the C-P bond would cause the appearance of a methanol peak, which was not observed. In further experiments, no decomposition of GD was detected on $[\text{Fe}_2\text{O}_3]\text{Al}_2\text{O}_3$ (Figure 2).

There was some evidence of GD decomposition of AP-CaO. The height of the P-F peak decreased slightly over 20 hours (Figure 2). This data are very different than the data reported by Wagner in a previous study. Wagner reported that >98% of GD had reacted in 24 h.⁵ Selected spectra for the reaction of GD on AP-CaO are provided in Figure 4a (t = 0 min) and Figure 5b (t = 240 min).

There was no evidence of mustard (characteristic absorbance bands at 1285 and 1212 cm^{-1}) decomposition on any of the adsorbents (kinetic data not provided). There was no increase in the characteristic absorption peak for TDG (expected mustard reaction product) at 1059 cm^{-1} . No evidence of the presence of chlorohydrin or sulfonium ion was seen. Each of these chemicals has one of its most intense bands in the area where TDG would have its strongest peaks. No peaks were present in the wavenumber range. The upscale peak for chlorohydrin ($\sim 3600 \text{ cm}^{-1}$) was also absent.

There was no evidence of VX (characteristic absorbance band at 1299 cm^{-1}) decomposition on any of the adsorbents (kinetic data not shown). There was no increase in the characteristic absorption peak for EMPA, EMPTA, or EA2192 (the expected hydrolysis products) at 1315, 1304, and 1204 cm^{-1} , respectively.

CONCLUSIONS

Transmission FTIR was used to determine the quasi-kinetic rates for the decomposition of chemical agents on metal oxide adsorbents. Non-standardized rates were reported as the decrease in height of a characteristic absorbance band versus time, and therefore, provided a comparison of reactivity for the adsorbents. Because the adsorbents affected the intensity of the agent absorbance spectra, a calibration curve would have been required for each reaction to determine true kinetic rates. With the inclusion of a calibration curve for each specific reaction, transmission FTIR could be used to determine reaction kinetics on paramagnetic adsorbents when MAS NMR is not possible.

Decomposition of GD occurred relatively fast on AP-MgO(1) and AP-MgO(2). When the reaction was repeated on MgO(1), no GD decomposition was detected. AP-MgO(1) appeared to have irreversibly degraded over several months. No reaction with either VX or HD was observed on AP-MgO(1), however, the reactions were run after the apparent degradation had occurred. Reactions including HD and VX were not done on AP-MgO(2).

There was insignificant decomposition of GD, HD, and VX on $[\text{Fe}_2\text{O}_3]\text{MgO}$, $[\text{Fe}_2\text{O}_3]\text{Al}_2\text{O}_3$, $[\text{CuO}]\text{Al}_2\text{O}_3$, and AP-CaO.

REFERENCES

1. FM 3-5, NBC Decontamination, July 2000
2. Klabunde, Kenneth J., Stark, Jane, Koper, Olga, Mohs, Cathy, Park, Dong G, Decker, Shawn, Jiang, Yan, Lagadic, Isabelle, and Zhang, Dajie, "Nanocrystals as Stoichiometric Reagents with Unique Surface Chemistry," J. Phys. Chem. Vol. 100, pp 12142-12153 (1996).
3. Klabunde, Kenneth J., and Mohs, Cathy, "Nanoparticles and Nanostructural Materials," Chapter 7, In Chemistry of Advanced Materials: An Overview, Wiley-VCH, Inc., Berlin, pp 271-327, 1998.
4. Mitchell, Mark B., Sheinker, V. N., and Mintz, Eric A., "Adsorption and Decomposition of Dimethyl Methylphosphonate on Metal Oxides," J. Phys. Chem. B, Vol. 101, (51), pp 11192-11203 (1997).
5. Wagner, George W., Bartram, Philip W., Koper, Olga, and Klabunde, Kenneth J., "Reactions of VX, GD, and HD with Nanosize MgO ," J. Phys. Chem. B, Vol. 103, (16), pp 3225-3228 (1999).

Figure 1. Decomposition of GD on Adsorbents as the Ratio of Product to GD Remaining

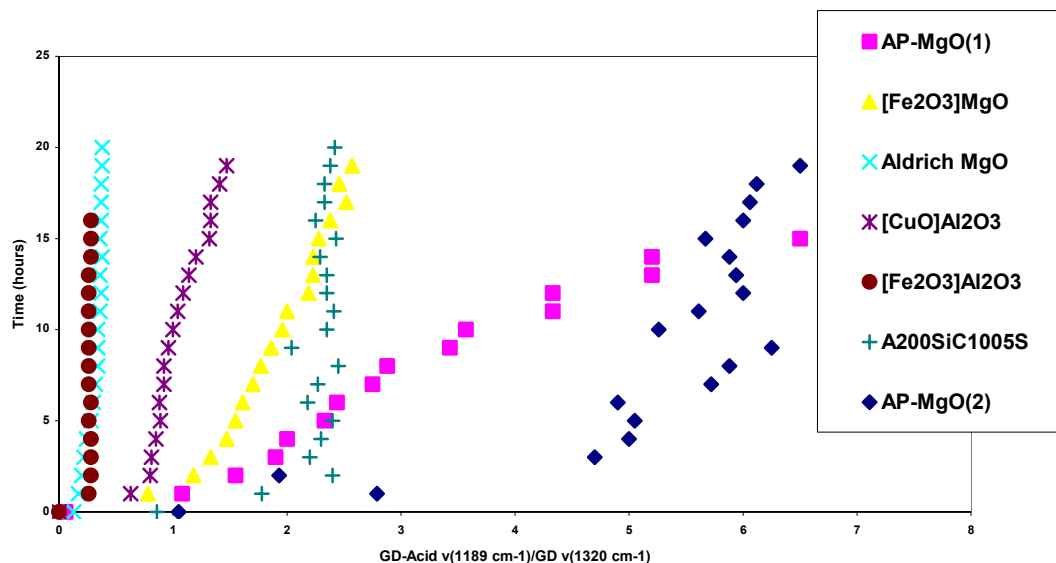


Figure 2. Decomposition of GD on Adsorbents as Determined by the Decrease in P-F Bond Absorbance

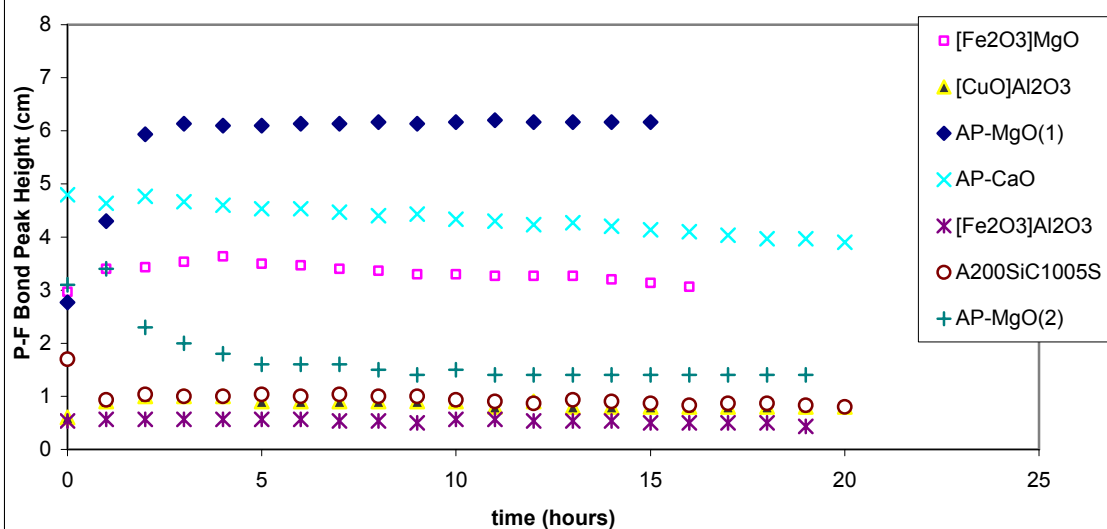


Figure 3a. Decomposition of GD on AP-MgO(1) (t = 0 min)

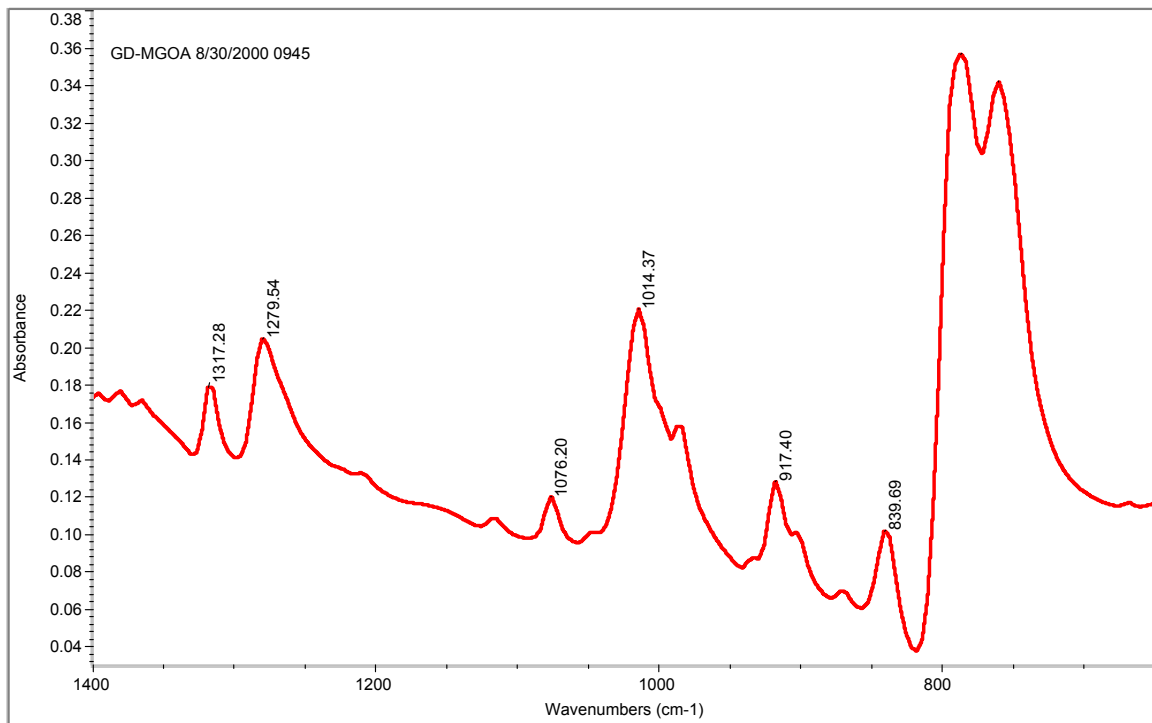


Figure 3b. Decomposition of GD on AP-MgO(1) (t = 240 min)

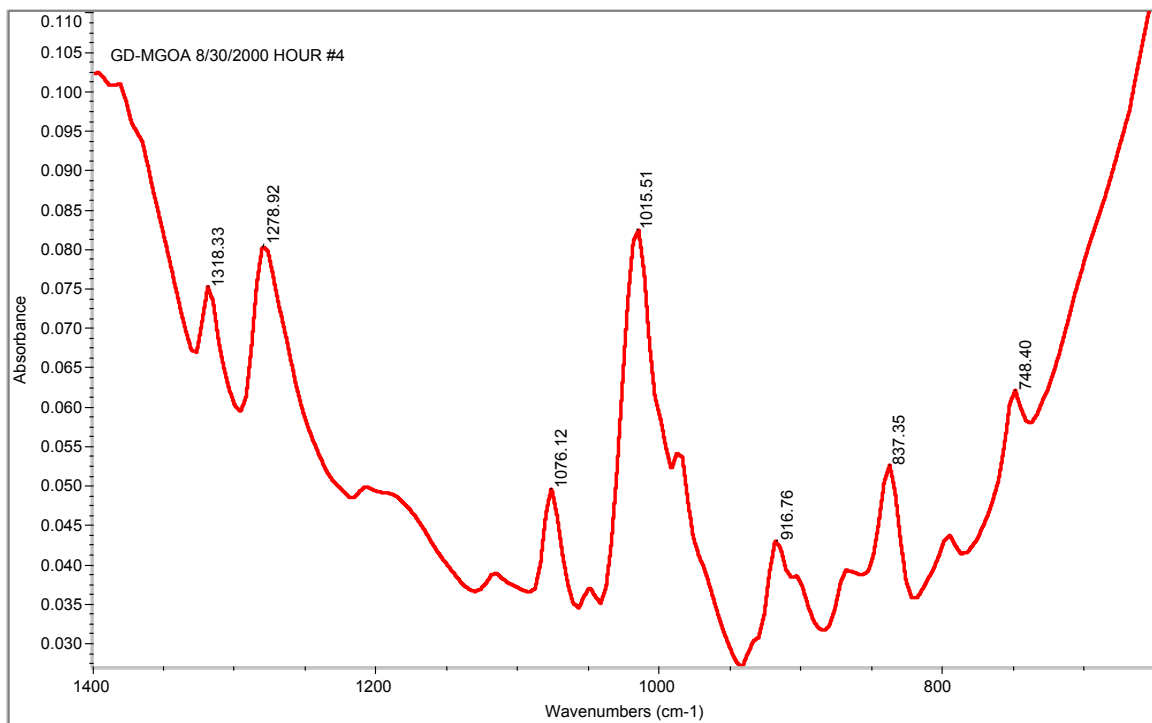


Figure 4a. Decomposition of GD on AP-CaO (t = 0 min)

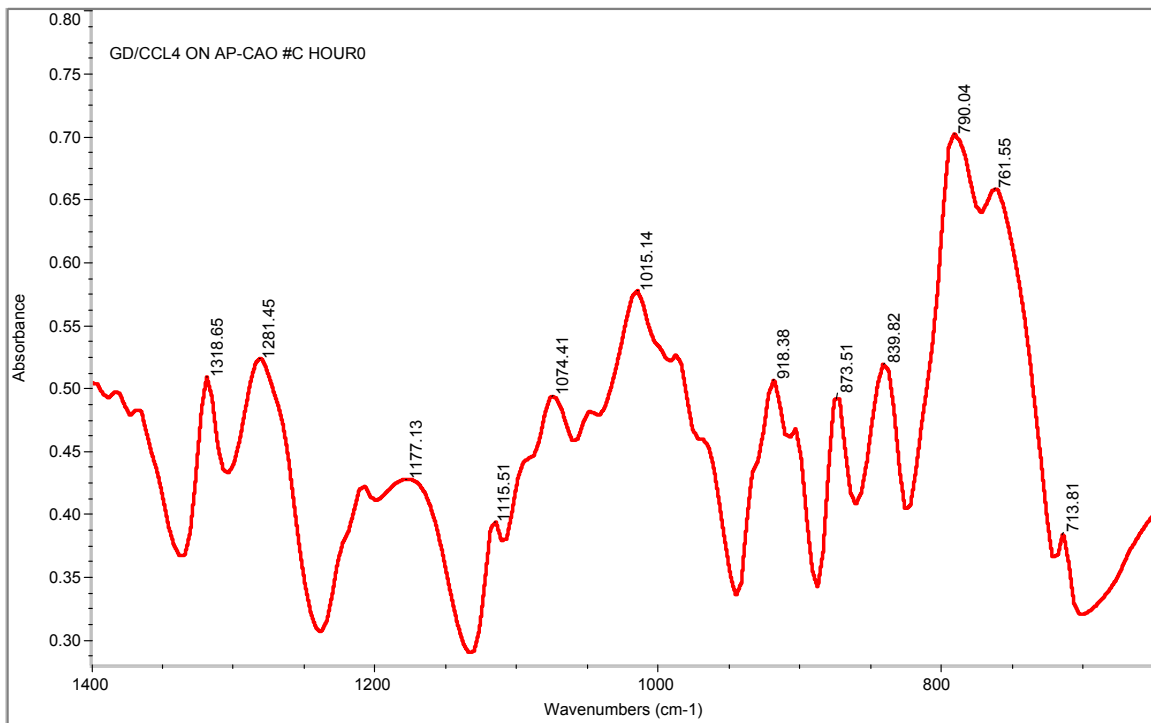


Figure 4b. Decomposition of GD on AP-CaO (t = 240 min)

